Proc. Natl. Acad. Sci. USA
Vol. 86, pp. 1619–1623, March 1989
Immunology

Human T cells expressing the γ/δ T-cell receptor (TcR-1): $C_\gamma 1$- and $C_\gamma 2$-encoded forms of the receptor correlate with distinctive morphology, cytoskeletal organization, and growth characteristics

(T-cell subsets/T-cell structure/cytoskeleton)

CARLO E. GROSSI*†, ERMANNO CICCONE*, NICOLA MIGONE‡, CRISTINA BOTTINO†, DANIELA ZARCONE†, MARIA C. MINGARI*§, SILVANO FERRINI*, GIUSEPPE TAMBUSSI†, ORIANE VIALE*, GIULIA CASORATI‡, ROMANO MILLO†, LORENZO MORETTA*§, AND ALESSANDRO MORETTA†¶

*Istituto Nazionale per la Ricerca sul Cancro, Genoa, Italy; §Istituto di Oncologia Clinica e Sperimentale, Universita' di Genova, Genoa, Italy; ‡Dipartimento di Genetica, Biologia e Chimica Medica, Universita' di Torino, Consiglio Nazionale delle Ricerche, Centro di Immunogenetica ed Istocompatibilita', Torino, Italy; and †Istituti di Istologia e di Anatomia Umana, Universita' di Genova, Genoa, Italy

Communicated by Renato Dulbecco, October 31, 1988 (received for review August 23, 1988)

ABSTRACT **BB3 and δ-TCS1 monoclonal antibodies identify two distinct nonoverlapping populations of T-cell receptor (TcR) γ/δ (TcR-1)-positive cells, which express a disulfide-linked and a nondisulfide-linked form of TcR, respectively. BB3$^+$ cells represented the majority of circulating TcR-1$^+$ cells, but they were virtually undetectable in the thymus. On the other hand, δ-TCS1$^+$ cells were largely predominant among TcR-1$^+$ thymocytes but represented a minority in peripheral blood (PB). Similar distributions were observed by clonal analysis of thymocytes or PB TcR-1$^+$ populations. The use of joining region (J)-specific probes indicated that BB3$^+$ and δ-TCS1$^+$ clones displayed different patterns of J rearrangement. Thus, the disulfide-linked form of TcR-1 (BB3$^+$ clones) was associated with the expression of J segments upstream to the $C_\gamma 1$ gene segment, whereas the nondisulfide-linked form (δ-TCS1$^+$ clones) was associated with the expression of J segments upstream to $C_\gamma 2$. δ-TCS1$^+$ clones, in most instances, exhibited a growth pattern different from that of BB3$^+$ or conventional TcR α/β^+ clones as they adhered promptly to surfaces, spread, and emitted long filopodia ending with adhesion plaques. Ultrastructural analyses showed, exclusively in δ-TCS1$^+$ cells, nuclear deformations, uropod formation, and abundant cytoskeletal structures. In addition, immunofluorescence studies of this subset of TcR-1$^+$ cells revealed the presence of abundant microtubules, intermediate filaments, and submembranous microfilaments. Thus, our findings suggest that δ-TCS1$^+$ cells are capable of active motility.**

In addition to conventional T lymphocytes expressing a receptor for antigen (TcR) composed of α and β chain (TcR-2) (1), another minor T-cell subset has been identified that expresses CD3-associated molecules represented by γ and δ chains (TcR-1) (2–8).

The availability of monoclonal antibodies (mAbs) directed against TcR-1 has allowed us to identify in the peripheral blood two distinct nonoverlapping populations of γ/δ TcR$^+$ cells (9). One cell population, accounting for ≈1/3rd of the total TcR-1$^+$ cells, expresses a nondisulfide-linked form of TcR-1 and reacts with the δ-TCS1 mAb. Cells of the other subset (≈2/3rd of the TcR-1$^+$ cells) bear a disulfide-linked form of TcR-1 and react with the BB3 mAb.

In this study, by analyzing large numbers of clones, we provide further evidence for the major molecular differences existing between the two types of cells expressing TcR-1. In addition, we provide direct evidence that the two TcR-1 isotypes are encoded by the $C_\gamma 1$ and $C_\gamma 2$ gene segments (C, constant region), respectively. Finally, we show that most δ-TCS1$^+$ (but not BB3$^+$) cells greatly differ from conventional TcR lymphocytes for their ability to grow as adherent cells and for the development and distribution of their cytoskeletal structures. These findings together with results of ultrastructural analyses suggest that δ-TCS1$^+$ cells may be endowed with peculiar motility properties.

MATERIALS AND METHODS

Cloning of CD3$^+$WT31$^-$ Peripheral Blood Lymphocytes or Thymocytes. Peripheral blood lymphocytes or thymocytes were prepared as described (9). CD3$^+$WT31$^-$ cells were subsequently isolated by fluorescence-activated cell sorting and cloned by limiting dilution in the presence of recombinant interleukin 2 (Cetus) (10).

mAbs and Flow Cytometry Analysis. mAbs used in these studies were the JT3A and Leu 4 (anti-CD3), B 9.4 (anti-CD8), WT31 (which recognizes TcR-2$^+$ cells), BB3, and δ-TCS1, which appear to recognize two different types of TcR γ/δ, and MAR 21 (anti-CD7).

Characterization of Radioiodinated Cell-Surface Proteins. Cloned cells (15×10^6) were surface-labeled with ^{125}I by the lactoperoxidase/glucose oxidase-catalyzed iodination method and lysed in a digitonin-containing buffer as described (9). Molecules immunoprecipitated from cell lysates by anti-CD3 mAb were analyzed on 11% SDS/polyacrylamide gels as described (8, 9).

DNA Analysis. The genomic configuration of three joining (J) segments (JP1, JP, and J1) upstream to $C_\gamma 1$ and the two segments (JP2 and J2) upstream to $C_\gamma 2$ were analyzed by Southern blotting, using different combinations of J-specific probes (11) and restriction endonucleases (*Eco*RI, *Bam*HI, and *Bgl* II). (For a detailed map of the TcR-γ region, see ref. 12.) Restriction enzyme analysis, Southern blot electrophoresis, and hybridization of ^{32}P-labeled nick-translated probes were performed as described (13). The assignment of specific variable region (*V*) genes to a given rearranged band was based on the use of *Eco*RI, *Bam*HI, and *Bgl* II restriction enzyme fragments as shown (14, 15).

Ultrastructural Analyses. For scanning electron microscopy (SEM) analyses, clonal microcultures of δ-TCS1$^+$ and

The publication costs of this article were defrayed in part by page charge payment. This article must therefore be hereby marked "*advertisement*" in accordance with 18 U.S.C. §1734 solely to indicate this fact.

Abbreviations: mAbs, monoclonal antibodies; MTOC, microtubule organizing center; SEM, scanning electron microscopy; TcR, T-cell receptor; C, J, and V, constant, joining, and variable regions.

¶To whom reprint requests should be addressed at: Istituto Nazionale per la Ricerca sul Cancro, Viale Benedetto XV, 10, 16132 Genoa, Italy.

Table 1. *V* gene involvement at the different J regions in TcR-1$^+$ clones

	JP1	JP	J1	JP2	J2
Group 1: Clones expressing disulfide-linked TcR-1					
66.1	V10	V9	G	G	G
R.12.4	V10	V9	G	G	G
5.25.10	d	V9	g	V11	G
6.25.4	d	V9	V2	G	G
S.25.B	d	V9	V2	G	G
D.15.50	d	V9	V3	G	G
12.S.9	d	V9	V8	G	G
Group 2: Clones expressing non-disulfide-linked TcR-1					
MV.28	d	d	d	d	V3, V8
MV.120	d	d	d	d	V3, V8
5.25.3	d	d	d	d	V8, V9
66.2	d	d	d	d	V3, V5
D.1.12	d	d	d	d	V3, V4

G, both alleles germ line; g, only one allele germ line; d, both alleles deleted.

BB3$^+$ cells were cultured for 3 days in flat-bottom 24-well culture plates (in the absence of feeder cells). Cells were subsequently fixed *in situ* with 3% glutaraldehyde in 0.1 M sodium cacodylate buffer (pH 7.3) overnight at 4°C. Subsequently, cells were dehydrated, critical point dried, and coated with gold. Specimens were examined with a Philips 505 scanning electron microscope.

For transmission electron microscopy analyses, cells fixed in suspension with 1.25% glutaraldehyde in 0.1 M cacodylate buffer (pH 7.5) for 1 hr at room temperature were washed, postfixed with 1% osmium tetroxide, dehydrated, and embedded in Spurr medium (16). Ultrathin sections stained with uranyl acetate/lead citrate were examined with a Philips EM301 electron microscope.

Localization of Cytoskeletal Components. Cytocentrifuge preparations of BB3$^+$ or δ-TCS1$^+$ cells (1×10^5) were fixed for 5 min at room temperature with 3% formaldehyde in phosphate-buffered saline (pH 7.6) supplemented with 2% sucrose, permeabilized with Triton X-100, 1% in Hepes buffer, and incubated with mouse mAbs anti-α- and anti-β-tubulin (Amersham) or anti-vimentin (Sanbio, Westbury, NY). As secondary reagent, we used goat anti-mouse immunoglobulins labeled with fluorescein isothiocyanate (FITC) (Southern Biotechnology Associates, Birmingham, AL). For the localization of microfilaments, a direct staining with FITC-labeled phalloidin (Sigma) was used.

RESULTS

Distribution of TcR-1$^+$ Cells in the Thymus and Peripheral Blood. As revealed by immunofluorescence studies, BB3$^+$ cells accounted for the majority of TcR-1$^+$ cells in unfractionated peripheral blood T cells but were virtually undetectable in the thymus cell preparations. On the other hand, cells expressing δ-TCS1 were consistently less than BB3$^+$ cells in peripheral blood but represented the majority of TcR-1$^+$ thymocytes. These differences were more evident when CD4$^-$CD8$^-$ cells (enriched in TcR-1$^+$ cells) were analyzed. It

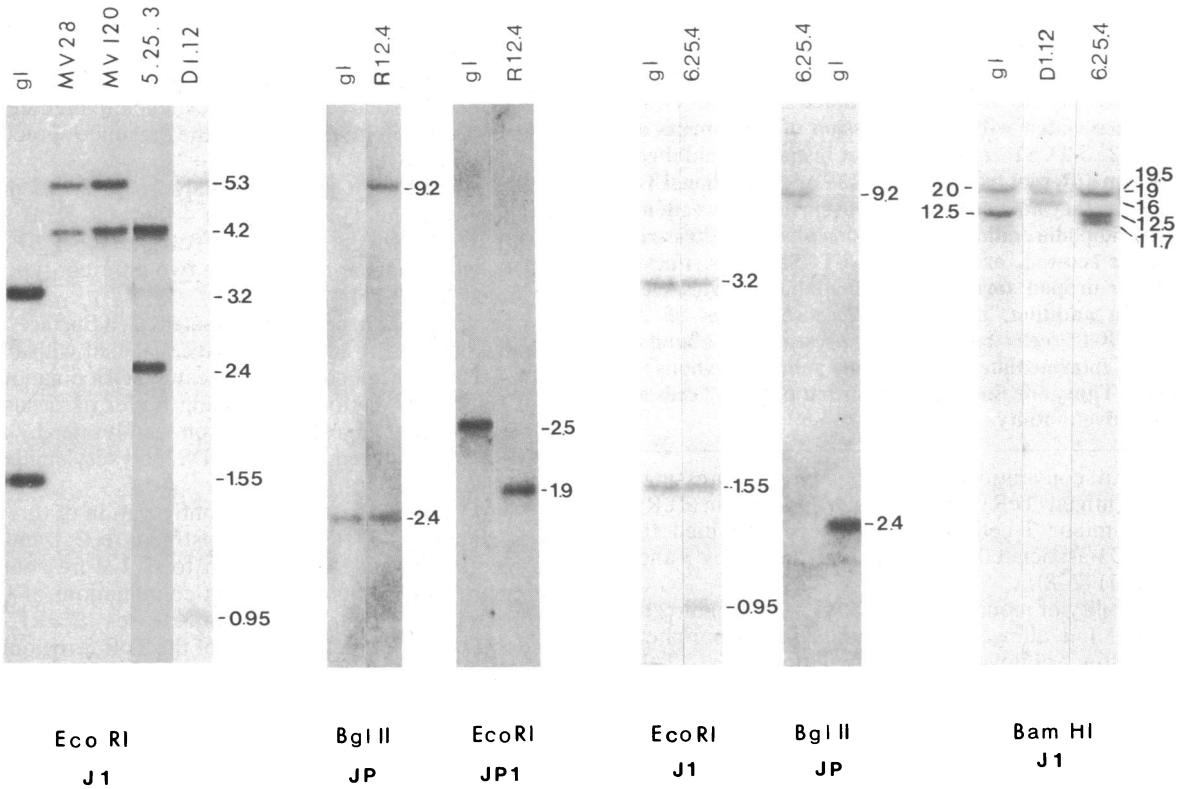

FIG. 1. Southern blot analysis of *Eco*RI-, *Bgl* II-, and *Bam*HI-digested DNA of representative cell clones expressing nondisulfide or disulfide-linked γ/δ receptors. DNA was hybridized to the J-specific probes as indicated. Lanes gl contain human fibroblast DNA showing the germ-line configuration of the J region. Due to their sequence homology, both the J1 and the J2 regions are detectable by the J1 probe: J1 is contained within the 1.55-kilobase (kb) *Eco*RI and 20-kb *Bam*HI germ-line fragments, whereas the J2 is detected within the 3.2-kb *Eco*RI and 12.5-kb *Bam*HI germ-line fragments. The *V* genes were assigned to the rearranged fragments as follows: JP1/*Eco*RI, 1.9-kb fragments to V10; JP/*Bgl* II, 9.2-kb fragment to V9 (this assignment was also confirmed by a JP/*Eco*RI analysis, where the expected 1.85-kb V9-containing fragment was found; data not shown); J1/*Eco*RI, 5.3-, 4.2-, 2.4-, and 0.95-kb fragments to V3, V8, V9, and V2 or V4, respectively; J1/*Bam*HI, 16-kb and 19.5-kb fragment to V3 and V9, respectively. Note that an identical 0.95-kb *Eco*RI fragment is produced by two different *V* genes (*V2* and *V4*) when rearranged either to J1 or J2. Therefore, samples showing such a band were analyzed with *Bam*HI. This enzyme, as shown in clones D1.12 and 6.25.4, can distinguish between V2 and V4, giving either a 19-kb V4-containing fragment or an 11.7-kb V2-containing band.

is of note that even in the $CD4^-CD8^-$ thymic cell preparations, which represent ≈1% of the total thymocyte population, $BB3^+$ cells were either undetectable or present in low proportions (<5%) (data not shown).

Molecular Heterogeneity of the TcR-1. $TcR\text{-}1^+$ clones were obtained from peripheral blood (or thymus). As previously shown, clones reacted with either BB3 or δ-TCS1 mAb (9). Moreover, immunoprecipitation experiments were performed in >20 $BB3^+$ clones and in 18 $\delta\text{-}TCS1^+$ clones. In agreement with our previous data (9), BB3-reactive TcR-1 molecules were represented by a major 80-kDa band, which, under reducing conditions, yielded two major components of ≈44 (δ) and 41 (γ) kDa and a minor component of 38 kDa (γ). In contrast, molecules immunoprecipitated from $\delta\text{-}TCS1^+$ clones displayed either a diffuse 41- to 44-kDa or (infrequently) a 55-kDa γ chain (17) under both reducing and nonreducing conditions (data not shown). Five $\delta\text{-}TCS1^+$ and seven $BB3^+$ clones were analyzed for the DNA configuration on the γ region by means of J-specific probes. The rearranged V–J segments in the examined clones are shown in Table 1. The disulfide-linked form of TcR-1 correlates with the rearrangement of the J segments upstream to the $C_\gamma 1$ gene region (JP1, JP, and J1) (Fig. 1). On the basis of the type of CD3-associated structures that were immunoprecipitated and because the transcripts of rearranged genes involving JP1, JP, and J1 segments are normally spliced to the $C_\gamma 1$ first exon, we can conclude that this panel of BB3-reactive clones utilize the $C_\gamma 1$ gene segments.

On the contrary, the nondisulfide-linked form of TcR-1 appears to be associated with the expression of J elements (J2 and JP2) immediately upstream to $C_\gamma 2$. The five $\delta\text{-}TCS1^+$ clones are likely to express the $C_\gamma 2$-encoded form of the γ chain, because the genomic region containing the $C_\gamma 1$ exons upstream to J2 has been deleted in both chromosomes (Fig. 1). To determine the *V* genes used by the clones examined, the size of the J bands was compared with that of all possible *V–J* combinations, according to the restriction enzyme maps of the *V* and the *J* gene families (14). It is of note that all clones using $C_\gamma 1$ show a V9–JP rearrangement (18).

***In Vitro* Growth Characteristics of $BB3^+$ and $\delta\text{-}TCS1^+$ Clones.** In the course of the clonal expansion of $TcR\text{-}1^+$ cells, we observed that, in a small number of clones, cells grew adherent and spread. With ongoing cell proliferation, the adherent cells occupied all the available surface of the U-bottom microwell and even climbed the walls of the culture well. A notable feature of these cells was the emission of extended filopodia (single or polar), which conferred to the cell a neuron-like appearance (Fig. 2). SEM analyses confirmed the unique morphological characteristics of these cells and showed the presence of adhesion plaques at the terminal end of each filopodium (Fig. 2). Phenotypic analyses revealed that all of the $TcR\text{-}1^+$ clones displaying these growth features had the $\delta\text{-}TCS1^+$ phenotype.

Cytoskeletal Organization of $BB3^+$ and $\delta\text{-}TCS1^+$ Clonal Cell Populations. The microtubule organizing center/centriole (MTOC) was demonstrated in all of the $BB3^+$ cells, but a microtubule radiation was barely detectable (Fig. 3*a*). In contrast, abundant microtubules were observed in $\delta\text{-}TCS1^+$ cells (Fig. 3*b*). These microtubules were organized as a radiation from the MTOC and developed as curved structures forming a perinuclear envelope. Although intermediate filaments were numerous in $BB3^+$ cells, they were clustered in a relatively small cytoplasmic area in the proximity of the nucleus (data not shown). In $\delta\text{-}TCS1^+$ cells, intermediate filaments were distributed along the major axis of the uropodia. These cells also contained more abundant intermediate filaments (data not shown). Actin was localized in the submembranous microfilaments, thus providing a pattern of peripheral fluorescent staining with phalloidin. Actin was concentrated in the axis of filopodia and microspikes, which conferred to some cells a "spiny" appearance. No actin stress fibers (19) were detected in both cell populations.

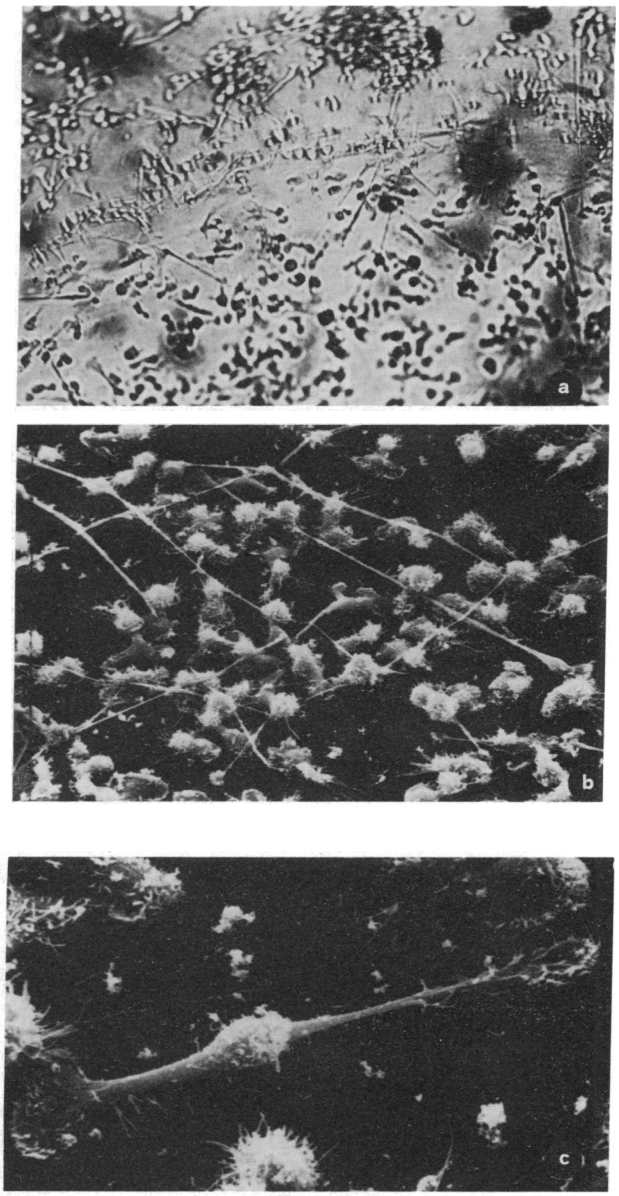

FIG. 2. Growth characteristics of $\delta\text{-}TCS1^+$ clones. (*a*) The edge of a culture as seen by inverted microscope shows cells adherent to the bottom (top) and cells climbing the walls of the culture well (bottom). (*b*) SEM analysis of the same culture; several cells show thin polar filopodia. (*c*) SEM observation at higher power demonstrates the presence of adhesion plaques at the terminal ends of polar filopodia. (*a*, ×80; *b*, ×550; *c*, ×1600.)

Ultrastructural Characteristics of $\delta\text{-}TCS1^+$ Clones. Clones with the $\delta\text{-}TCS1^+$ phenotype also displayed a high degree of morphologic uniformity and their ultrastructural features were markedly different from those of $BB3^+$ cells. Bizarre cellular shapes were detectable also in ultrathin sections. Uropod formation was a constant feature for most $\delta\text{-}TCS1^+$ cells and sections of filopodia were occasionally seen (Fig. 3 *c* and *d*). Nuclei were highly irregular in shape, with deep clefts and indentations, and frequently they exhibited a cerebriform Sézary-like morphology. The cytoplasm, largely confined to the uropod region, contained numerous electron-dense granules and abundant microtubules, intermediate filaments, and submembranous microfilaments. The latter cytoskeletal structures were also organized to form the axis of filopodia.

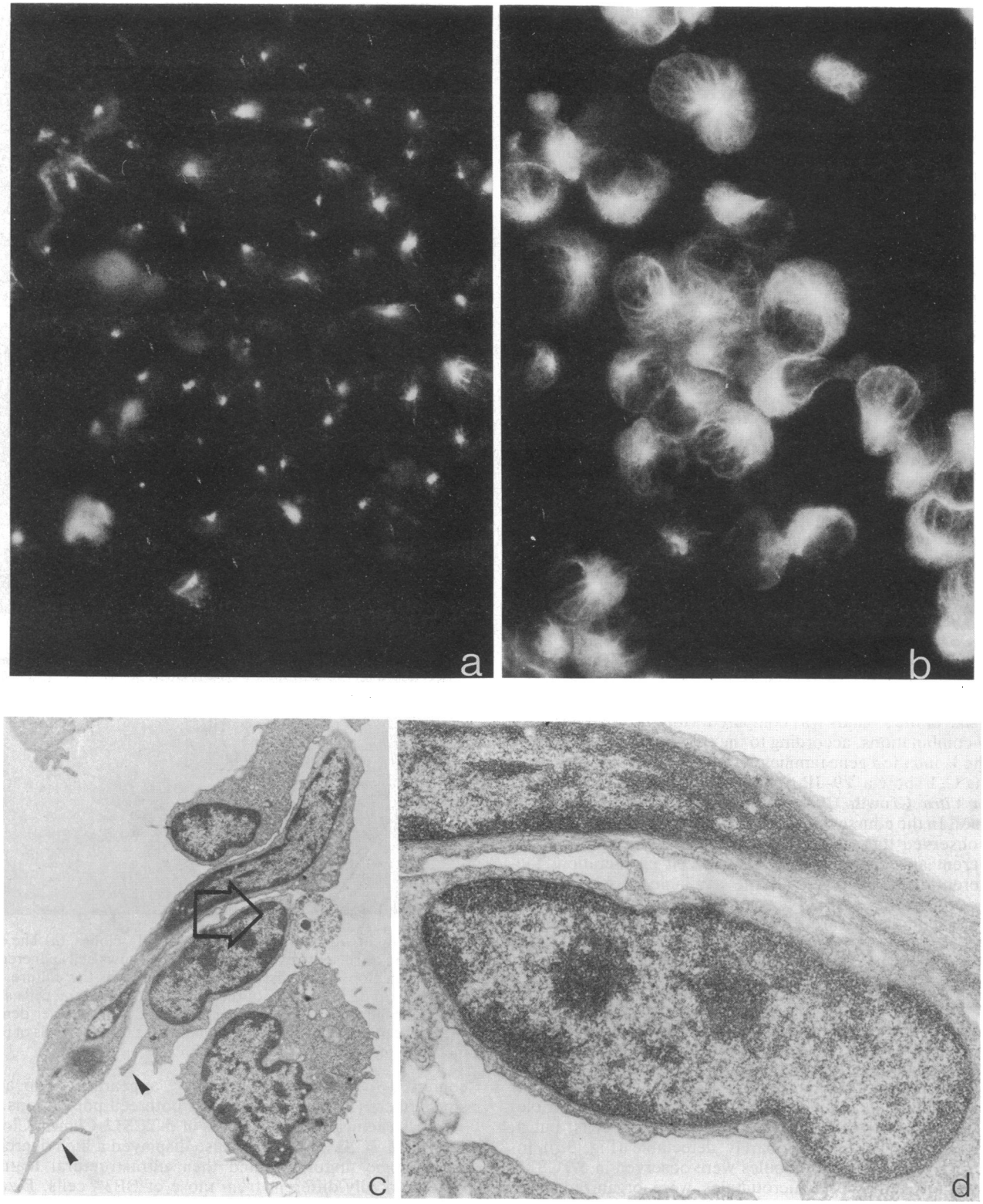

FIG. 3. Immunofluorescence localization of α- and β-tubulins and ultrastructural features of human TcR-1$^+$ cells. (*a*) In a BB3$^+$ clone, the MTOCs are present in all of the cells, but the microtubular radiation is barely visible. (*b*) In a δ-TCS1$^+$ clone, an extended microtubular radiation convergent on the MTOCs is present in all of the cells. (*c*) In δ-TCS1$^+$ clones, most cells show irregular nuclear shapes, uropod formation, and abundant electron-dense granules. A bizarre cell (arrow), apparently binucleate, is shown. A thin cytoplasmic bridge (shown in *d*) connects two distinct territories of the same cell, each of them comprised of nucleus and cytoplasm. Arrowheads in *c* indicate sections of filopodia. (*c*, ×4900; *d*, ×24,000.)

DISCUSSION

In this study we provide further evidence that, by using appropriate mAbs against TcR-1, two distinct subsets of TcR-1$^+$ cells can be identified (9, 17). Thus, at both the population and the clonal level, BB3$^+$ and δ-TCS1$^+$ cells belong to two nonoverlapping TcR-1$^+$ subsets.

Analyses of the distribution of TcR-1$^+$ cells in the peripheral blood and in the thymus revealed a predominance of BB3$^+$ cells in the circulation, whereas δ-TCS1$^+$ cells were

largely predominant in the thymus (9). In addition to the definition of two TcR-1$^+$ cell subsets, expression of BB3 or δ-TCS1 mAbs was found to be associated with distinct molecular forms of the receptor (9). Thus, all the BB3$^+$ clones analyzed expressed a CD3-associated, disulfide-linked, heterodimer, whereas δ-TCS1$^+$ clones always expressed a nondisulfide-linked form of the TcR-1. Interestingly, the δ-TCS1-reactive nondisulfide-linked form of TcR-1 appeared to consist of two different molecular sizes—i.e., a "heavy" form of ≈55 kDa and another form of 41–44 kDa (17).

Previous studies have provided evidence that two distinct C_γ gene segments are used by TcR-1$^+$ cells (11). On the basis of the amino acid sequences, it has been proposed that $C_\gamma 1$, but not $C_\gamma 2$, molecular products can form interchain disulfide bonds (20, 21). Here we provide direct evidence that BB3$^+$ cells expressing the disulfide-linked form of the TcR-1 utilize the $C_\gamma 1$ gene segment and that a $C_\gamma 2$ gene rearrangement occurs in δ-TCS1$^+$ cells expressing the nondisulfide-linked form of TcR-1.

In a minority of the expanding clones, we could observe an early adherence of the cells to the surface, with cell spreading, uropod formation, and the emission of long polar filopodia with adhesion plaques at their terminal ends. These cells appeared actively motile in culture. Phenotypic analyses revealed that all of these clones were δ-TCS1$^+$.

Immunofluorescence localization of cytoskeletal proteins (α- and β-tubulin, vimentin, and actin) showed marked differences in the amount and distribution of cytoskeletal components. Thus, only δ-TCS1$^+$ cells displayed an extended microtubular radiation originating from the MTOCs and developing around the nucleus. Consistent with the abundance of the microtubular radiation was the finding of intermediate filaments that "decorated" the whole cytoplasmic area, particularly in the uropod region where they were organized to form axial structures and were also found in the proximity of the cell membrane. Submembranous actin was more abundant in δ-TCS1$^+$ cells than in BB3$^+$ cells and was also located in the axis of filopodia and microspikes.

Ultrastructural analyses demonstrated that δ-TCS1$^+$ cells display several morphologic features of actively motile cells. These features comprised a variety of nuclear shapes, from cerebriform to deeply cleft, uropod formation, and the emission of filopodia and microspikes. This, in turn, suggests that δ-TCS1$^+$ cells might have unique homing features for migration into tissues rather than the property of circulating in the bloodstream. In this context, the recent finding that TcR-1$^+$ cells are present in the intestinal epithelium and in the epidermis of both mice and humans may be important (22–25).

We are grateful to Dr. W. Malorni (Istituto Superiore di Sanita', Rome) who performed SEM analyses. This work was supported by grants from the National Research Council of Italy, Progetto Finalizzato Oncologia, to C.E.G., M.C.M., and L.M., and from the Italian Association for Cancer Research (AIRC) to C.E.G., L.M. and A.M.; O.V. and G.C. are recipients of an AIRC fellowship.

1. Acuto, O. & Reinherz, E. L. (1985) *N. Engl. J. Med.* **312,** 100–111.
2. Brenner, M. B., McLean, J., Dialynas, D. P. B., Strominger, J. L., Smith, J. A., Owen, F. L., Seidman, J. G., Ip, S., Rosen, F. & Krangel, M. S. (1986) *Nature (London)* **322,** 145–149.
3. Brenner, M. B., McLean, J., Scheft, H., Riberdy, J., Ang, S. L., Seidman, J. G., Devlin, P. & Krangel, M. S. (1987) *Nature (London)* **325,** 689–694.
4. Borst, J., Van de Griend, R. J., Oostveen, J. M., Ang, S. L., Melief, C. J., Seidman, J. G. & Bolhuis, R. L. H. (1987) *Nature (London)* **325,** 683–688.
5. Moingeon, P., Ythier, A., Goubin, G., Faure, F., Novill, A., Delmon, L., Reinaud, M., Forestier, F., Daffos, F., Bohuon, C. & Hercend, T. (1986) *Nature (London)* **323,** 638–640.
6. Sowder, J. T., Chen, C. H., Ager, L. L., Chan, M. M. & Cooper, M. D. (1988) *J. Exp. Med.* **167,** 315–321.
7. Chen, C. H., Cihak, J., Losch, V. & Cooper, M. D. (1988) *Eur. J. Immunol.* **18,** 539–543.
8. Ciccone, E., Ferrini, S., Bottino, C., Viale, O., Prigione, I., Pantaleo, G., Tambussi, G., Moretta, L. & Moretta, A. (1988) *J. Exp. Med.* **167,** 1517–1527.
9. Bottino, C., Tambussi, G., Ferrini, S., Ciccone, E., Varese, P., Mingari, M. C., Moretta, L. & Moretta, A. (1988) *J. Exp. Med.* **168,** 491–505.
10. Moretta, A., Pantaleo, G., Moretta, L., Cerottini, J. C. & Mingari, M. C. (1983) *J. Exp. Med.* **157,** 743–754.
11. Lefranc, M. P. & Rabbitts, T. H. (1985) *Nature (London)* **316,** 464–466.
12. Lefranc, M. P., Forster, A. & Rabbitts, T. H. (1986) *Proc. Natl. Acad. Sci. USA* **83,** 9596–9600.
13. Migone, N., Feder, J., Cann, H., van West, B., Hwang, J., Takahashi, N., Honjo, T., Piazza, A. & Cavalli-Sforza, L. L. (1983) *Proc. Natl. Acad. Sci. USA* **80,** 467–471.
14. Forster, A., Huck, S., Ghanem, N., Lefranc, M. P. & Rabbitts, T. H. (1987) *EMBO J.* **6,** 1945–1950.
15. Migone, N., Casorati, G., Francia di Celle, P., Lusso, P., Foa, R. & Lefranc, M. P. (1986) *Eur. J. Immunol.* **18,** 173–178.
16. Spurr, A. T. (1969) *J. Ultrastruct. Res.* **26,** 31–43.
17. Moretta, A., Bottino, C., Ciccone, E., Tambussi, G., Mingari, M. C., Ferrini, S., Casorati, G., Varese, P., Viale, O., Migone, N. & Moretta, L., *J. Exp. Med.*, in press.
18. Triebel, F., Lefranc, M. P. & Hercend, T. (1988) *Eur. J. Immunol.* **18,** 789–794.
19. Byers, H. R. & Fujiwara, K. (1982) *J. Cell Biol.* **93,** 804–811.
20. Pelicci, P. G., Subar, M., Weiss, A., Dalla-Favera, R. & Littman, D. R. (1987) *Science* **237,** 1051–1054.
21. Littman, D. R., Newton, M., Crommie, D., Ang, S. L., Seidman, J. G., Gettner, S. N. & Weiss, A. (1987) *Nature (London)* **326,** 85–88.
22. Bonyhardi, M., Weiss, A., Tucker, P. W., Tigelaar, R. E. & Allison, J. P. (1987) *Nature (London)* **330,** 574–576.
23. Goodman, T. & Lefrancois, L. (1988) *Nature (London)* **333,** 855–858.
24. Janeway, C. A. (1988) *Nature (London)* **333,** 804–806.
25. Foster, C. A., Yokoseky, H., Groh, V., Rieger, A., Kofler, G., Koning, F., Brenner, M. B. & Stingh, G. (1988) *J. Invest. Dermatol.* **90,** 560A.